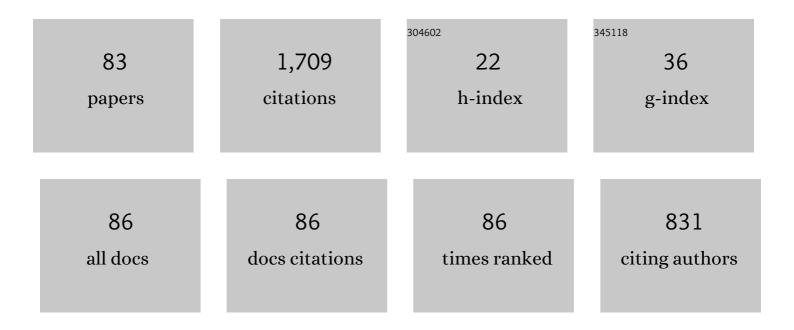
## Lidong Dai

List of Publications by Year in descending order

Source: https://exaly.com/author-pdf/6741267/publications.pdf Version: 2024-02-01



#	Article	IF	CITATIONS
1	Pressure-induced coupled structural–electronic transition in SnS <sub>2</sub> under different hydrostatic environments up to 39.7 GPa. RSC Advances, 2022, 12, 2454-2461.	1.7	12
2	Some Remarks on the Electrical Conductivity of Hydrous Silicate Minerals in the Earth Crust, Upper Mantle and Subduction Zone at High Temperatures and High Pressures. Minerals (Basel, Switzerland), 2022, 12, 161.	0.8	6
3	Pressure-Induced Structural Phase Transition and Metallization of CrCl <sub>3</sub> under Different Hydrostatic Environments up to 50.0 GPa. Inorganic Chemistry, 2022, 61, 4852-4864.	1.9	14
4	Effect of Different Mineralogical Proportions on the Electrical Conductivity of Dry Hot-Pressed Sintering Gabbro at High Temperatures and Pressures. Minerals (Basel, Switzerland), 2022, 12, 336.	0.8	1
5	Experimental Research on Electrical Conductivity of the Olivine-Ilmenite System at High Temperatures and High Pressures. Frontiers in Earth Science, 2022, 10, .	0.8	2
6	Constraints on fluids in the continental crust from laboratory-based electrical conductivity measurements of plagioclase. Gondwana Research, 2022, 107, 1-12.	3.0	7
7	High-Temperature and High-Pressure Phase Transition of Natural Barite Investigated by Raman Spectroscopy and Electrical Conductivity. Frontiers in Earth Science, 2022, 10, .	0.8	1
8	High-pressure investigations on the isostructural phase transition and metallization in realgar with diamond anvil cells. Geoscience Frontiers, 2021, 12, 1031-1037.	4.3	8
9	High-pressure structural phase transition and metallization in Ga <sub>2</sub> S <sub>3</sub> under non-hydrostatic and hydrostatic conditions up to 36.4 CPa. Journal of Materials Chemistry C, 2021, 9, 2912-2918.	2.7	20
10	Pressure-Induced Structural Phase Transition and Metallization in Ga2Se3 Up to 40.2 GPa under Non-Hydrostatic and Hydrostatic Environments. Crystals, 2021, 11, 746.	1.0	3
11	Pressure-induced structural phase transitions in natural kaolinite investigated by Raman spectroscopy and electrical conductivity. American Mineralogist, 2021, , .	0.9	7
12	Pressure-induced metallic phase transition in gallium arsenide up to 24.3 GPa under hydrostatic conditions. Modern Physics Letters B, 2021, 35, .	1.0	3
13	Electrical properties of dry polycrystalline olivine mixed with various chromite contents: Implications for the high conductivity anomalies in subduction zones. Geoscience Frontiers, 2021, 12, 101178.	4.3	7
14	Thermal Ionization of Hydrogen in Hydrous Olivine With Enhanced and Anisotropic Conductivity. Journal of Geophysical Research: Solid Earth, 2021, 126, e2021JB022939.	1.4	7
15	Influence of Saline Fluids on the Electrical Conductivity of Olivine Aggregates at High Temperature and High Pressure and Its Geological Implications. Frontiers in Earth Science, 2021, 9, .	0.8	3
16	Electrical Conductivity of Tiâ€Bearing Hydrous Olivine Aggregates at High Temperature and High Pressure. Journal of Geophysical Research: Solid Earth, 2020, 125, e2020JB020309.	1.4	14
17	Electrical Conductivity of Clinopyroxeneâ€NaClâ€H 2 O System at High Temperatures and Pressures: Implications for Highâ€Conductivity Anomalies in the Deep Crust and Subduction Zone. Journal of Geophysical Research: Solid Earth, 2020, 125, e2019JB019093.	1.4	15
18	The Phase Transition and Dehydration in Epsomite under High Temperature and High Pressure. Crystals, 2020, 10, 75.	1.0	11

LIDONG DAI

#	Article	IF	CITATIONS
19	The Elastic Properties of β-Mg2SiO4 Containing 0.73 wt.% of H2O to 10 GPa and 600 K by Ultrasonic Interferometry with Synchrotron X-Radiation. Minerals (Basel, Switzerland), 2020, 10, 209.	0.8	4
20	An Overview of the Experimental Studies on the Electrical Conductivity of Major Minerals in the Upper Mantle and Transition Zone. Materials, 2020, 13, 408.	1.3	12
21	Experimental study on the electrical properties of carbonaceous slate: a special natural rock with unusually high conductivity at high temperatures and pressures. High Temperatures - High Pressures, 2020, 48, 439-454.	0.3	2
22	Electrical conductivities of minerals and rocks in the Earth crust, upper mantle, mantle transition zone and subduction zone. Acta Geologica Sinica, 2019, 93, 120-121.	0.8	1
23	Characterization of metallization and amorphization for GaP under different hydrostatic environments in diamond anvil cell up to 40.0 GPa. Review of Scientific Instruments, 2019, 90, 066103.	0.6	24
24	Characterization of the pressure-induced phase transition of metallization for MoTe2 under hydrostatic and non-hydrostatic conditions. AIP Advances, 2019, 9, 065104.	0.6	15
25	Structural Phase Transition and Metallization of Nanocrystalline Rutile Investigated by High-Pressure Raman Spectroscopy and Electrical Conductivity. Minerals (Basel, Switzerland), 2019, 9, 441.	0.8	11
26	Pressure-induced phase transitions for goethite investigated by Raman spectroscopy and electrical conductivity. High Pressure Research, 2019, 39, 106-116.	0.4	13
27	Effect of Temperature, Pressure, and Chemical Composition on the Electrical Conductivity of Schist: Implications for Electrical Structures under the Tibetan Plateau. Materials, 2019, 12, 961.	1.3	5
28	Evidences for phase transition and metallization in β-In2S3 at high pressure. Chemical Physics, 2019, 524, 63-69.	0.9	7
29	Phase Transition and Metallization of Orpiment by Raman Spectroscopy, Electrical Conductivity and Theoretical Calculation under High Pressure. Materials, 2019, 12, 784.	1.3	10
30	Influence of High Conductive Magnetite Impurity on the Electrical Conductivity of Dry Olivine Aggregates at High Temperature and High Pressure. Minerals (Basel, Switzerland), 2019, 9, 44.	0.8	14
31	Pressure-induced phase transitions of ZnSe under different pressure environments. AIP Advances, 2019, 9, .	0.6	21
32	Pressure-induced metallization in MoSe <sub>2</sub> under different pressure conditions. RSC Advances, 2019, 9, 5794-5803.	1.7	26
33	Effect of temperature, pressure and chemical composition on the electrical conductivity of granulite and geophysical implications. Journal of Mineralogical and Petrological Sciences, 2019, 114, 87-98. Pressure-induced irreversible metallization accompanying the phase transitions in <mml:math< td=""><td>0.4</td><td>3</td></mml:math<>	0.4	3
34	xmlns:mml="http://www.w3.org/1998/Math/MathML"> <mml:mrow><mml:mi mathvariant="normal"&gt;S<mml:msub><mml:mi mathvariant="normal"&gt;S<mml:mn>2</mml:mn></mml:mi </mml:msub><mml:msub><mml:mi mathvariant="normal"&gt;S<mml:mn>3</mml:mn></mml:mi </mml:msub></mml:mi </mml:mrow> .	1.1	45
35	Physical Review B, 2018, 97, . Deviatoric stresses promoted metallization in rhenium disulfide. Journal Physics D: Applied Physics, 2018, 51, 165101.	1.3	15
36	Migration of impurity level reflected in the electrical conductivity variation for natural pyrite at high temperature and high pressure. Physics and Chemistry of Minerals, 2018, 45, 85-92.	0.3	10

LIDONG DAI

#	Article	IF	CITATIONS
37	Single crystal growth, characterization and high-pressure Raman spectroscopy of impurity-free magnesite (MgCO3). Physics and Chemistry of Minerals, 2018, 45, 423-434.	0.3	17
38	High–pressure electrical conductivity and Raman spectroscopy of chalcanthite. Spectroscopy Letters, 2018, 51, 531-539.	0.5	5
39	Pressure-induced reversible metallization and phase transition in Zinc Telluride. Modern Physics Letters B, 2018, 32, 1850342.	1.0	6
40	Effect of chemical composition on the electrical conductivity of gneiss at high temperatures and pressures. Solid Earth, 2018, 9, 233-245.	1.2	10
41	Effect of dehydrogenation on the electrical conductivity of Fe-bearing amphibole: Implications for high conductivity anomalies in subduction zones and continental crust. Earth and Planetary Science Letters, 2018, 498, 27-37.	1.8	55
42	Pressure-induced structural phase transition and dehydration for gypsum investigated by Raman spectroscopy and electrical conductivity. Chemical Physics Letters, 2018, 706, 151-157.	1.2	11
43	Effect of dehydration on the electrical conductivity of phyllite at high temperatures and pressures. Mineralogy and Petrology, 2017, 111, 853-863.	0.4	14
44	Anomalous phase transition of Bi-doped Zn2GeO4 investigated by electrical conductivity and Raman spectroscopy under high pressure. Journal of Applied Physics, 2017, 121, 125901.	1.1	12
45	Influence of dehydration on the electrical conductivity of epidote and implications for highâ€conductivity anomalies in subduction zones. Journal of Geophysical Research: Solid Earth, 2017, 122, 2751-2762.	1.4	45
46	Pressure-induced permanent metallization with reversible structural transition in molybdenum disulfide. Applied Physics Letters, 2017, 110, .	1.5	45
47	Electrical conductivity of mudstone (before and after dehydration at high P-T) and a test of high conductivity layers in the crust. American Mineralogist, 2017, 102, 2450-2456.	0.9	16
48	Pressure-induced irreversible amorphization and metallization with a structural phase transition in arsenic telluride. Journal of Materials Chemistry C, 2017, 5, 12157-12162.	2.7	35
49	Experimental Study on the Electrical Conductivity of Pyroxene Andesite at High Temperature and High Pressure. Pure and Applied Geophysics, 2017, 174, 1033-1041.	0.8	6
50	The Influence of Dehydration on the Electrical Conductivity of Trachyandesite at High Temperatures and High Pressures. Journal of Materials Science and Engineering A, 2017, 7, .	0.0	0
51	Influence of temperature, pressure, and oxygen fugacity on the electrical conductivity of dry eclogite, and geophysical implications. Geochemistry, Geophysics, Geosystems, 2016, 17, 2394-2407.	1.0	35
52	Raman scattering of 2 <i>H</i> -MoS2 at simultaneous high temperature and high pressure (up to 600 K) Tj ETQq	0 0 0 rgBT	- /&verlock 1
53	Erratum to "Reply to comment on â€~High and highly anisotropic electrical conductivity of the asthenosphere due to hydrogen diffusion in olivine' by Dai and Karato [Earth Planet. Sci. Lett. 408 (2014) 79–86]―[Earth Planet. Sci. Lett. 427 (2015) 300–302]. Earth and Planetary Science Letters, 2016, 454, 319.	1.8	Ο

Pressure-induced phase-transition and improvement of the microdielectric properties in yttrium-doped SrZrO <sub>3</sub>. Europhysics Letters, 2016, 114, 56003.

0.7 9

Lidong Dai

#	Article	IF	CITATIONS
55	Pressure-induced improvement of grain boundary properties in yttrium-doped BaZrO <sub>3</sub> . Journal Physics D: Applied Physics, 2016, 49, 345102.	1.3	7
56	Evidence of the pressure-induced conductivity switching of yttrium-doped SrTiO <sub>3</sub> . Journal of Physics Condensed Matter, 2016, 28, 475501.	0.7	22
57	Experimental study on the electrical conductivity of quartz andesite at high temperature and high pressure: evidence of grain boundary transport. Solid Earth, 2015, 6, 1037-1043.	1.2	14
58	Electrical conductivity of gabbro: the effects of temperature, pressure and oxygen fugacity. European Journal of Mineralogy, 2015, 27, 215-224.	0.4	16
59	Temperature and pressure dependence of electrical conductivity in synthetic anorthite. Solid State lonics, 2015, 276, 136-141.	1.3	22
60	Reply to comment on "High and highly anisotropic electrical conductivity of the asthenosphere due to hydrogen diffusion in olivine―by Dai and Karato [Earth Planet. Sci. Lett. 408 (2014) 79–86]. Earth and Planetary Science Letters, 2015, 427, 300-302.	1.8	5
61	Electrical conductivity of hydrous natural basalts at high temperatures and pressures. Journal of Applied Geophysics, 2015, 112, 290-297.	0.9	12
62	Influence of temperature, pressure, and chemical composition on the electrical conductivity of granite. American Mineralogist, 2014, 99, 1420-1428.	0.9	29
63	The effect of pressure on the electrical conductivity of olivine under the hydrogen-rich conditions. Physics of the Earth and Planetary Interiors, 2014, 232, 51-56.	0.7	39
64	Influence of oxygen fugacity on the electrical conductivity of hydrous olivine: Implications for the mechanism of conduction. Physics of the Earth and Planetary Interiors, 2014, 232, 57-60.	0.7	35
65	Influence of FeO and H on the electrical conductivity of olivine. Physics of the Earth and Planetary Interiors, 2014, 237, 73-79.	0.7	35
66	High and highly anisotropic electrical conductivity of the asthenosphere due to hydrogen diffusion in olivine. Earth and Planetary Science Letters, 2014, 408, 79-86.	1.8	91
67	Electrical conductivity of K-feldspar at high temperature and high pressure. Mineralogy and Petrology, 2014, 108, 609-618.	0.4	28
68	Electrical conductivity of alkali feldspar solid solutions at high temperatures and high pressures. Physics and Chemistry of Minerals, 2013, 40, 51-62.	0.3	38
69	Electrical conductivity of Alm82Py15Grs3 almandine-rich garnet determined by impedance spectroscopy at high temperatures and high pressures. Tectonophysics, 2013, 608, 1086-1093.	0.9	24
70	Sound velocities of Na0.4Mg0.6Al1.6Si0.4O4 NAL and CF phases to 73ÂGPa determined by Brillouin scattering method. Physics and Chemistry of Minerals, 2013, 40, 195-201.	0.3	18
71	The effect of chemical composition and oxygen fugacity on the electrical conductivity of dry and hydrous garnet at high temperatures and pressures. Contributions To Mineralogy and Petrology, 2012, 163, 689-700.	1.2	50
72	Electrical conductivity of albite at high temperatures and high pressures. American Mineralogist, 2011, 96, 1821-1827.	0.9	29

LIDONG DAI

#	Article	IF	CITATIONS
73	The electrical conductivity of dry polycrystalline olivine compacts at high temperatures and pressures. Mineralogical Magazine, 2010, 74, 849-857.	0.6	36
74	Novel technique to control oxygen fugacity during high-pressure measurements of grain boundary conductivities of rocks. Review of Scientific Instruments, 2009, 80, 033903.	0.6	14
75	Electrical conductivity of wadsleyite at high temperatures and high pressures. Earth and Planetary Science Letters, 2009, 287, 277-283.	1.8	99
76	Comments on "Electrical conductivity of wadsleyite as a function of temperature and water content― by Manthilake et al Physics of the Earth and Planetary Interiors, 2009, 174, 19-21.	0.7	51
77	Electrical conductivity of pyrope-rich garnet at high temperature and high pressure. Physics of the Earth and Planetary Interiors, 2009, 176, 83-88.	0.7	100
78	Electrical conductivity of orthopyroxene: Implications for the water content of the asthenosphere. Proceedings of the Japan Academy Series B: Physical and Biological Sciences, 2009, 85, 466-475.	1.6	115
79	In-situ control of different oxygen fugacity experimental study on the electrical conductivity of Iherzolite at high temperature and high pressure. Journal of Physics and Chemistry of Solids, 2008, 69, 101-110.	1.9	12
80	Experimental study of grain boundary electrical conductivities of dry synthetic peridotite under highâ€ŧemperature, highâ€pressure, and different oxygen fugacity conditions. Journal of Geophysical Research, 2008, 113, .	3.3	40
81	Experimental measurement of the electrical of the electrical conductivity of single crystal olivine at high temperature and high pressure under different oxygen fugacities *. Progress in Natural Science: Materials International, 2006, 16, 387-393.	1.8	8
82	Some New Progress in the Experimental Measurements on Electrical Property of Main Minerals in the Upper Mantle at High Temperatures and High Pressures. , 0, , .		1
83	High-pressure structural phase transitions and metallization in layered HfS <sub>2</sub> under different hydrostatic environments up to 42.1 GPa. Journal of Materials Chemistry C. 0	2.7	10